

# High-efficiency calculation of elastic constants enhanced by the optimized strain-matrix sets

Zhong-Li Liu\*

*College of Physics and Electric Information, Luoyang Normal University, Luoyang 471934, China*

(Dated: February 4, 2020)

Elastic constants are of fundamental importance to multi-discipline and engineering. Although the stress-strain method is computationally expensive based on the density functional theory, it is much easier and straightforward to implement. Especially at high pressure, it does not need complex pressure corrections like the energy-strain method. We here report the optimized high efficiency strain-matrix sets (OHES) used in the stress-strain method to determine the full second-order elastic constants of materials belonging to any crystal system in either three or two dimensional. For the three kinds of strain matrix sets tested, we performed extensive comparison on the accuracy and efficiency for different materials in all crystal systems. We find that our proposed OHES has much higher efficiency than the other two when ensuring the same level of computation accuracy. In future, the OHES will tremendously improve the computational efficiency of elastic constants in either the exploration of materials' properties or high-throughput new materials design.

Keywords: Elastic constant; Hooke's law; Density functional theory; Strain-matrix set

## I. INTRODUCTION

Elastic constants are fundamental parameters from which we start to understand the physical and even chemical properties of crystal materials. They reflect the mechanical response characteristics of materials to external forces and loads applied in different manners, and hence provide useful information on the strength and even the hardness of materials (See Ref.<sup>1</sup> and references therein). The velocities of elastic waves in materials intimately correlates with elastic constants and then the systematic acoustic properties of materials can be deduced consequently. Thus, especially the elastic constants of mineral materials provide key information for understanding the characteristics of the seismic wave when traveling through Earth's interior<sup>2</sup>. Elastic constants can also help the analysis of materials' thermodynamic properties, such as phonon dispersion relation, thermal expansion, Debye temperature, Grüneisen parameter and melting temperature<sup>3</sup>. On the atomic scale, elastic constants directly reflect the strength of chemical bonding in materials along different orientations<sup>4</sup>. Therefore, elastic constants strongly concern physics, condensed matter, materials science, geophysics, chemical, and even engineering.

Elastic constants are traditionally measured by experiment. While, till now not all materials' elastic constants are available experimentally. Fortunately, the high-accuracy state of the art density functional theory (DFT)<sup>5,6</sup> has already paved the way for achieving elastic constants reliably. At high pressure, it is especially difficult for experiment to directly measure elastic constants, and then the DFT based elastic constants calculations are of vital importance in both the exploration of materials' properties and new materials design. In the computer-aided new materials design, such as crystal structure prediction<sup>7-12</sup>, elastic constants are frequently calculated and utilized to check the stability of the predicted struc-

tures according to Born elastic stability criteria<sup>13-18</sup>. Moreover, for the new materials design based on the materials informatics, elastic constants are extensively calculated and collected in materials database, such as the Materials Project (MP) database<sup>19</sup>.

Elastic constants can be calculated by either the energy-strain or stress-strain method (See Refs.<sup>20-22</sup> and references therein). The former usually needs relatively lower computation accuracy of energy but larger number of strain sets. While, the latter depends on much higher accuracy of stress tensors but smaller number of strain sets<sup>20,21</sup>. In the latter method, the high accuracy of stress tensors calculation always need higher energy cutoff and denser K-point meshes, and thus are much more computationally expensive and time-consuming. But comparatively it is much easier to implement according to Hooke's law. Especially, it is straightforward to calculate high pressure/temperature elastic constants using the stress-strain method. On the contrary, the energy-strain method need rather complex pressure corrections for the obtained elastic constants<sup>23</sup>.

For the stress-strain method, Yu and coauthors proposed the universal linear-independent coupling strains (ULICS) to couple all the stress components together for extracting the complete set of elastic constants simultaneously<sup>18</sup>. While coupling of stress components by adding several strain components at the same time in the ULICS will largely reduce the symmetry of strained crystal. This will greatly lengthen the computation time using DFT calculations. The calculations of elastic constants have been implemented in several previous work<sup>18,20-22</sup>. We here optimized the strain matrix sets of deformations applied on any crystal system including three-dimension (3D) and two-dimension (2D) to keep the symmetry of crystal under deformation to the most extent, and consequently improve the computation efficiency considerably.

The rest of this paper is arranged as follows. The the-

ory of elastic constants calculation and the optimization of strain matrix sets are presented in Sec. II. The test and comparison of computation accuracy and efficiency of different strain matrix sets are detailed in Sec. III. Section IV describes our further discussions and the final conclusions.

## II. METHODOLOGY

### A. Elasticity theory

The elastic properties of a material uncover the characteristics of the response to external loads applied in different manners. According to Hooke's law, the stresses  $\sigma_i$  in a crystal are in proportional to the corresponding strains  $\varepsilon_j$  within the linear elastic regime,

$$\sigma_i = \sum_{j=1}^6 C_{ij} \varepsilon_j \quad (1)$$

where the proportional coefficient  $C_{ij}$  are the elastic stiffness constants of the crystal. Equation (1) uses the Voigt notation<sup>24</sup> in which 1, 2, ..., and 6 represent  $xx, yy, zz, yz, zx, xy$ , respectively. In the computational determination of elastic constants, for the given strain sets of a crystal the stress tensors can be calculated either by empirical atomic potential methods or more accurately by first-principles methods.

In the 3D bulk case, the strain matrix can be written in the following form

$$\varepsilon = \begin{bmatrix} \varepsilon_1 & \varepsilon_6/2 & \varepsilon_5/2 \\ \varepsilon_6/2 & \varepsilon_2 & \varepsilon_4/2 \\ \varepsilon_5/2 & \varepsilon_4/2 & \varepsilon_3 \end{bmatrix}. \quad (2)$$

For the 2D layered case, we assume that the crystal plane lies in the  $xy$  plane and the strain matrix is simplified as

$$\varepsilon = \begin{bmatrix} \varepsilon_1 & \varepsilon_6/2 & 0 \\ \varepsilon_6/2 & \varepsilon_2 & 0 \\ 0 & 0 & 0 \end{bmatrix}. \quad (3)$$

Then the deformation matrix applied to the crystal unit cell matrix is

$$\mathbf{D} = \mathbf{I} + \varepsilon, \quad (4)$$

where  $\mathbf{I}$  is the  $3 \times 3$  unit matrix. The crystal lattice vector with deformation is

$$\mathbf{A}' = \mathbf{A} \cdot \mathbf{D} \quad (5)$$

where  $\mathbf{A}$  is the crystal lattice vector without deformation.

For various crystal systems, there are different numbers of second order elastic constants (SOECs) reduced from the full 21 (3D) or 6 (2D) elastic constants thanks to their lattice symmetries. The numbers of the SOECs for different lattice symmetries are listed in Table I.

TABLE I. The numbers of the SOECs of different symmetries for 3D and 2D lattices. SGN means the space group number of crystal structures. Dim. is abbreviated for dimensional.

Dim.	Crystal system	SGN	Number	Prototype
3D	Cubic	195-230	3	C, Al, CsCl
	Hexagonal	168-194	5	Os, Ti, TiB <sub>2</sub>
	Rhombohedral I	149-167	6	Al <sub>2</sub> O <sub>3</sub>
	Rhombohedral II	143-148	7	CaMg(CO <sub>3</sub> ) <sub>2</sub>
	Tetragonal I	89-142	6	MgF <sub>2</sub>
	Tetragonal II	75-88	7	CaMoO <sub>4</sub>
	Orthorhombic	16-74	9	TiSi <sub>2</sub>
	Monoclinic	3-15	13	ZrO <sub>2</sub>
	Triclinic	1-2	21	ReS <sub>2</sub>
2D	Hexagonal	-	2	Graphene, MoS <sub>2</sub>
	Square	-	3	FeSe
	Rectangular	-	4	Phosphorene, AuSe
	Oblique	-	6	-

### B. Optimization of strain matrix sets

Yu *et al.* proposed the ULICS to couple all the stress components together, making it possible to extract the complete set of elastic constants simultaneously<sup>18</sup>. While, after full tests we found that the deformations applied to the crystal lattice vectors using the ULICS sets largely lower the symmetries of crystals and in consequence greatly increase the computational cost, especially for the DFT method, as will be shown in Section III. In order to optimize the strain matrix sets and finally lower the computational cost by keeping higher symmetries of crystal to the most extent, we here introduce the optimized high efficiency strain-matrix sets (OHES). The OHES uses the least number of strain matrix sets to solve the corresponding elastic constants numerically. As the tests shown in Section III, the calculation efficiency is largely improved compared to the ULICS.

As for the details of the ULICS, the readers are referred to Ref.<sup>18</sup>. The detailed OHES of different lattice systems belonging to both 3D and 2D lattice systems are listed in Table II. Certain elastic constants can be deduced from the corresponding certain strain sets. For comparison, we also employed the all single-element strain-matrix sets (ASESS) to test the accuracy and efficiency of elastic constant computations. Contrary to the ULICS, the ASESS largely decouple the stress components in calculations. The full ASESS and corresponding derived elastic constants are listed in Table III. Table IV compares the numbers of strain matrix sets used for the ASESS, the OHES and the ULICS. The numbers of the OHES are almost identical to those of the ULICS, except for the monoclinic structure, i.e., the OHES use less number of strain matrix sets than the ULICS.

TABLE II. The full OHES of different lattice system belonging to 3D and 2D crystals. Different elastic constants can be derived from different strain matrices. Dim. is abbreviated for dimensional.

Dim.	Lattice system	Number of matrix	$\epsilon_1$	$\epsilon_2$	$\epsilon_3$	$\epsilon_4$	$\epsilon_5$	$\epsilon_6$	Derived $C_{ij}$
3D	Cubic	1	$\delta$	0	0	$\delta$	0	0	$C_{11}, C_{12}, C_{44}$
		2	$\delta$	0	0	0	0	0	$C_{11}, C_{12}, C_{13}$
	Hexagonal	2	0	0	$\delta$	$\delta$	0	0	$C_{33}, C_{44}$
		2	$\delta$	0	0	0	0	0	$C_{11}, C_{12}, C_{13}, C_{14}$
	Rhombohedral I	2	0	0	$\delta$	$\delta$	0	0	$C_{33}, C_{44}$
		2	$\delta$	0	0	0	0	0	$C_{11}, C_{12}, C_{13}, C_{14}, C_{15}$
	Rhombohedral II	2	0	0	$\delta$	$\delta$	0	0	$C_{33}, C_{44}$
		2	$\delta$	0	0	0	0	0	$C_{11}, C_{12}, C_{13}$
	Tetragonal I	2	0	0	$\delta$	$\delta$	0	0	$C_{33}, C_{44}$
		2	$\delta$	0	0	0	0	0	$C_{11}, C_{12}, C_{13}, C_{16}$
	Tetragonal II	2	0	0	$\delta$	$\delta$	0	0	$C_{33}, C_{44}$
		3	$\delta$	0	0	0	0	0	$C_{11}, C_{12}, C_{13}$
	Orthorhombic	3	0	$\delta$	0	0	0	0	$C_{22}, C_{23}$
		4	0	0	$\delta$	$\delta$	$\delta$	$\delta$	$C_{33}, C_{44}, C_{55}, C_{66}$
	Monoclinic	4	$\delta$	0	0	0	0	0	$C_{11}, C_{12}, C_{13}, C_{16}$
4		0	$\delta$	0	0	0	0	$C_{22}, C_{23}, C_{26}$	
Triclinic	6	0	0	$\delta$	$\delta$	0	0	$C_{33}, C_{36}, C_{44}, C_{45}$	
	6	0	0	0	0	$\delta$	$\delta$	$C_{55}, C_{66}$	
Triclinic	6	$\delta$	0	0	0	0	0	$C_{11}, C_{12}, C_{13}, C_{14}, C_{15}, C_{16}$	
	6	0	$\delta$	0	0	0	0	$C_{22}, C_{23}, C_{24}, C_{25}, C_{26}$	
Triclinic	6	0	0	$\delta$	0	0	0	$C_{33}, C_{34}, C_{35}, C_{36}$	
	6	0	0	0	$\delta$	0	0	$C_{44}, C_{45}, C_{46}$	
Triclinic	6	0	0	0	0	$\delta$	0	$C_{55}, C_{56}$	
	6	0	0	0	0	0	$\delta$	$C_{66}$	
2D	Hexagonal	1	$\delta$	0	0	0	0	$\delta$	$C_{11}, C_{12}$
	Square	1	$\delta$	0	0	0	0	$\delta$	$C_{11}, C_{12}, C_{66}$
	Rectangular	2	$\delta$	0	0	0	0	$\delta$	$C_{11}, C_{12}, C_{66}$
		2	0	$\delta$	0	0	0	0	$C_{22}$
	Oblique	3	$\delta$	0	0	0	0	0	$C_{11}, C_{12}, C_{16}$
		3	0	$\delta$	0	0	0	0	$C_{22}, C_{26}$
Oblique	3	0	0	0	0	0	$\delta$	$C_{33}$	

TABLE III. The full ASESS of different lattice system belonging to 3D and 2D crystals. Different elastic constants can be derived from different strain matrices. NM means the number of matrices.

System	NM	$\epsilon_1$	$\epsilon_2$	$\epsilon_3$	$\epsilon_4$	$\epsilon_5$	$\epsilon_6$	Derived $C_{ij}$
Any 3D	6	$\delta$	0	0	0	0	0	$C_{11}, C_{12}, C_{13}, C_{14}, C_{15}, C_{16}$
		0	$\delta$	0	0	0	0	$C_{22}, C_{23}, C_{24}, C_{25}, C_{26}$
		0	0	$\delta$	0	0	0	$C_{33}, C_{34}, C_{35}, C_{36}$
		0	0	0	$\delta$	0	0	$C_{44}, C_{45}, C_{46}$
		0	0	0	0	$\delta$	0	$C_{55}, C_{56}$
		0	0	0	0	0	$\delta$	$C_{66}$
Any 2D	3	$\delta$	0	0	0	0	0	$C_{11}, C_{12}, C_{16}$
		0	$\delta$	0	0	0	0	$C_{22}, C_{26}$
		0	0	0	0	0	$\delta$	$C_{66}$

### C. The calculation details of stress tensors

Before the calculations of elastic constants, each crystal structure was first fully optimized at ambient pressure. Then after atomic positions were fully relaxed when the crystal lattice is under specific deformations applied according to OHES, ASESS, or ULICS, the stress

TABLE IV. Comparison of the numbers of strain matrix sets used for ASESS, OHES and ULICS. Dim. is abbreviated for dimensional.

Dim.	Lattice system	ASESS	OHES	ULICS
3D	Cubic	6	1	1
	Hexagonal	6	2	2
	Rhombohedral	6	2	2
	Tetragonal	6	2	2
	Orthorhombic	6	3	3
	Monoclinic	6	4	5
	Triclinic	6	6	6
2D	Hexagonal	3	1	1
	Square	3	1	1
	Rectangular	3	2	2
	Oblique	3	3	3

components were calculated accurately. The relaxations guarantee forces acting on each atom to be less than 0.001 eV/Å. All the structural optimization and stress computations in this work are performed using the projector augmented wave (PAW) method<sup>25</sup> as implemented in the Vienna ab initio simulation package (VASP)<sup>26,27</sup>. In all

calculations, we employ the Perdew, Becke and Ernzerhof (PBE)<sup>28</sup> generalized gradient approximation (GGA) for the exchange-correlation functional. The energy cut-off values for all materials were set to ensure energy to be converged to  $10^{-6}$  eV. For all three kinds of strain matrix sets, the OHES, ULICS, and ASESS, we used exactly the same parameters for elastic constants calculations. To derive elastic constants, the values  $-0.06$ ,  $-0.03$ ,  $0.0$ ,  $0.03$ , and  $0.06$  of  $\delta$  in these strain matrix sets were adopted for the first order polynomial fitting according to Eq.1. Accordingly, these values were also taken in the ULICS as the largest strain value for comparison. It is noted that such small  $\delta$  in the magnitude of  $10^{-3}$  proposed by Yu et al.<sup>18</sup> are not applicable in some cases because of numerical noises.

### III. RESULTS AND DISCUSSIONS

Utilizing the three kinds of strain sets, the OHES, the ASESS, and the ULICS, we fully optimized the prototype materials listed in Table I and calculated their elastic constants with VASP. The prototype materials belong to different crystal systems in either 3D or 2D. Just like the comparisons shown in the following subsection III A, the OHES, the ASESS, and the ULICS have almost the same accuracy in calculating the elastic constants of the listed prototype materials. However, the OHES has overall the highest efficiency compared with the ASESS and ULICS, as shown in subsection III B. In the following two subsections, we will intensively compare the accuracy and efficiency of the three strain sets in both 3D and 2D.

#### A. Accuracy comparison of elastic constants from different strain sets

We calculated the elastic constants of the prototype materials listed in Table I using the OHES, the ULICS, and the ASESS, and made a detailed comparison of their accuracy for different crystal systems. As shown in Table I, the 3D prototype materials are mainly divided into the cubic, the hexagonal, the rhombohedral, the tetragonal, the orthorhombic, the monoclinic, and the triclinic system. The prototype materials cover the range of the ionic crystals, covalent crystals, and metals. The tests and comparisons were also extended to 2D materials.

##### 1. Three dimensional materials

We first tested the computation accuracy of the three kinds of strain sets in calculating the elastic constants for 3D crystals ranging from high-symmetry systems (the cubic) to the low-symmetry systems (the monoclinic). For the cubic system, we took the diamond, Al, and CsCl as examples and the calculated elastic constants are listed in Table.V, in comparison with the materials project

(MP)<sup>19</sup> data and experimental data. The tested crystal types covered the covalent, metallic, and ionic crystals. It is seen that the elastic constants from the three kinds of strain sets are all in good agreement with the corresponding MP data<sup>19</sup> and experimental values<sup>19,29,30</sup>. The comparison for Al is also illustrated in Fig.1. It is noted that the OHES results have almost the same computation accuracy with the ULICS and ASESS.

TABLE V. The elastic constants calculated by the OHES, ULICS and ASESS for the cubic prototype systems, in comparison with MP values and experimental data.

System	Method	$C_{11}$	$C_{12}$	$C_{44}$
Diamond	OHES	1055.0	136.6	567.8
	ULICS	1063.4	145.0	582.1
	ASESS	1054.2	131.3	566.3
	MP <sup>19</sup>	1054	126	562
	Exp. <sup>29</sup>	1077.0	124.6	577.0
Al	OHES	115.3	62.1	36.6
	ULICS	104.6	70.0	34.2
	ASESS	114.1	62.1	31.6
	MP <sup>19</sup>	104	73	32
	Exp. <sup>31</sup>	108.0	62.0	28.3
CsCl	OHES	33.4	5.9	5.5
	ULICS	33.4	6.7	6.4
	ASESS	33.0	5.5	5.0
	MP <sup>19</sup>	34	6	5
	Exp. <sup>30</sup>	36.4	8.8	8.0

TABLE VI. The calculated elastic constants of the hexagonal systems together with the MP data and experimental values.

System	Method	$C_{11}$	$C_{12}$	$C_{13}$	$C_{33}$	$C_{44}$
Os	OHES	768.8	238.9	231.4	858.4	265.4
	ULICS	747.9	243.3	238.2	855.4	258.8
	ASESS	768.8	241.3	225.2	850.1	256.7
	MP <sup>19</sup>	730	226	220	824	252
	Exp. <sup>32</sup>	763.3	227.9	218.0	843.2	269.3
Ti	OHES	172.8	92.3	84.4	189.4	38.2
	ULICS	173.2	91.5	84.9	185.0	38.5
	ASESS	172.8	91.9	84.5	191.8	39.4
	MP <sup>19</sup>	177	83	76	191	42
	Exp. <sup>33</sup>	160	90	66	181	46
TiB <sub>2</sub>	OHES	660.8	77.7	120.1	473.6	267.3
	ULICS	658.4	80.5	125.1	474.9	264.5
	ASESS	660.8	77.1	116.9	470.1	261.4
	MP <sup>19</sup>	642	75	106	443	258
	Exp. <sup>34</sup>	660	48	93	432	260

For the hexagonal systems, we calculated the elastic constants of hcp Os, Ti and TiB<sub>2</sub> using the three kinds of strain sets, OHES, ASESS, and ULICS. The results are shown in Table VI., in which the MP data<sup>19</sup> and the experimental data<sup>32-34</sup> are also listed. Good agreement is also found for the hexagonal systems between our calculated elastic constants and the MP data and the corresponding experiments. The comparison for Os is also illustrated in Fig.1. The results indicate the three kinds

of strain sets produce almost the same accuracy of the elastic constant of the hexagonal systems, compared with experimental data<sup>32–34</sup>.

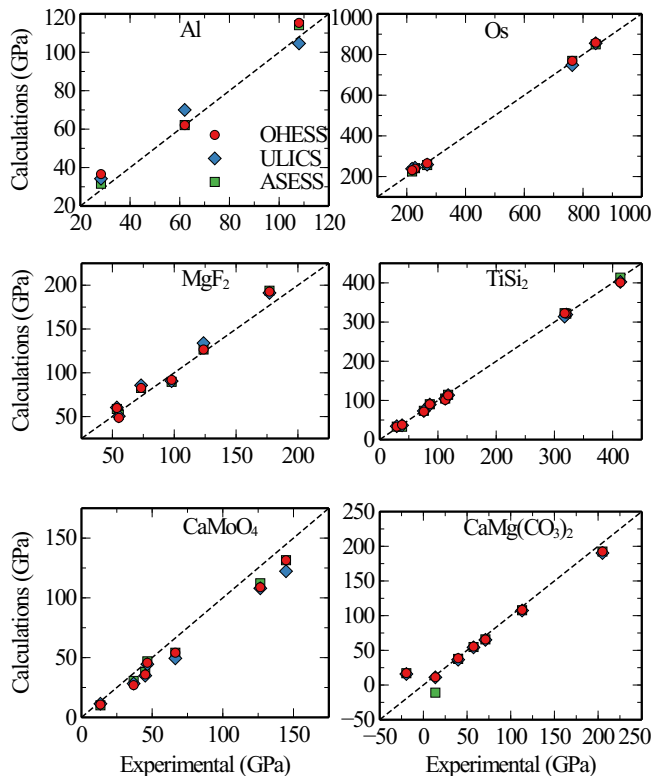


FIG. 1. Comparison of the elastic constants from OHESS, ACESS and ULICS with experiments

We listed the calculated elastic constants of the rhombohedral and tetragonal systems in Table VII. For the trigonal system,  $\text{Al}_2\text{O}_3$  and  $\text{CaMg}(\text{CO}_3)_2$  belong to rhombohedral I and II as listed in Table I, respectively.  $\text{MgF}_2$  and  $\text{CaMoO}_4$  fall into the tetragonal I and II crystal systems, respectively. The obtained elastic constants of the two crystal systems using OHESS and ULICS and ACESS are in good agreement with the corresponding MP data<sup>19</sup> and experimental values<sup>33,35–37</sup>. The negative values of some elastic constant are resulted from the ‘-’ Cartesian coordinate system defined in Ref.<sup>21</sup>. The absolute values of the calculated negative elastic constants are also in agreement with those of the MP data and experimental values. The accuracy comparison of the elastic constants for  $\text{MgF}_2$ ,  $\text{CaMoO}_4$  and  $\text{CaMg}(\text{CO}_3)_2$  are also shown in Fig. 1. The OHESS strain sets produced almost the same results compared with ULICS and ACESS.

The test examples for the orthorhombic and monoclinic crystal systems are  $\text{TiSi}_2$  and  $\text{ZrO}_2$  respectively. The calculated elastic constants are shown in Table VIII. The agreement of calculated elastic constants for orthorhombic  $\text{TiSi}_2$  with the MP data and experimental values is reasonably good, while the agreement for monoclinic  $\text{ZrO}_2$  is not. The worse agreement for  $\text{ZrO}_2$  probably can be attributed to the low accuracy of the stresses

calculated by VASP in such a low symmetry of monoclinic structure.

We take the triclinic  $\text{ReS}_2$  as the lowest-symmetry 3D case for comparing the computation accuracy of the OHESS, ULICS, and ACESS. The calculated elastic constants of  $\text{ReS}_2$  are presented in Table IX. We note that for the triclinic crystal system the OHESS is the same with ACESS and they have the same six strain matrices, as shown in Table II and III. Therefore, just as shown in Table IX the calculated elastic constants are exactly the same values for OHESS and ACESS. For the detailed comparison, we find that all the elastic constants from the ULICS are in good accordance with those from OHESS and ACESS correspondingly.

## 2. Two-dimensional layered materials

We have also tested the accuracy of the elastic constant calculations for 2D crystals using the three strain sets, OHESS, ULICS and ACESS. Our calculated results and others’ theoretical values are compared in Table X. Once again, we found a good agreement of our calculated results with others’ calculations<sup>20,40</sup>. More importantly, the OHESS results are also in good agreement with the ULICS and ACESS results.

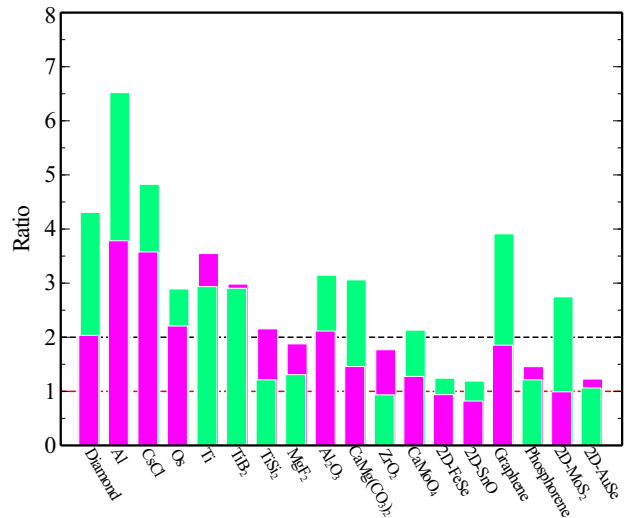


FIG. 2. The ratios of the total computational time used by ULICS (pink) and ACESS (green) to that used by OHESS for calculating elastic constants of different crystals in 3D and 2D.

## B. Computation efficiency of different strain sets

Although the OHESS has almost the same order of accuracy with ULICS and ACESS in all the calculations, we should compare the time that they used for calculating elastic constants and find the most efficient one. All

TABLE VII. The calculated elastic constants of the (Al<sub>2</sub>O<sub>3</sub> and CaMg(CO<sub>3</sub>)<sub>2</sub>) and tetragonal (MgF<sub>2</sub> and CaMoO<sub>4</sub>) systems compared with the MP data and experimental values.

System	Method	$C_{11}$	$C_{12}$	$C_{13}$	$C_{14}$	$C_{15}$	$C_{16}$	$C_{33}$	$C_{44}$	$C_{66}$
CaMg(CO <sub>3</sub> ) <sub>2</sub>	OHESS	192.4	65.7	55.4	17.2	11.3		108.3	38.6	
	ULICS	190.3	65.1	54.3	15.9	11.1		107.4	36.5	
	ASESS	192.4	65.8	54.8	17.0	-11.0		107.8	37.6	
	MP <sup>19</sup>	192	65	55	17	11		108	37	
CaMoO <sub>4</sub>	Exp. <sup>35</sup>	205.0	71.0	57.4	-19.5	13.7		113.0	39.8	
	OHESS	131.5	54.1	45.7			10.7	108.9	27.0	35.9
	ULICS	122.3	49.4	44.5			11.4	108.0	28.3	34.9
	ASESS	131.5	54.1	46.9			10.1	112.2	30.5	37.9
	MP <sup>19</sup>	133	56	47			-12	113	29	37
Al <sub>2</sub> O <sub>3</sub>	Exp. <sup>36</sup>	144.7	66.4	46.6			13.4	126.5	36.9	45.1
	OHESS	448.1	154.3	111.6	19.8			454.1	131.9	
	ULICS	449.3	150.2	111.0	20.1			452.4	130.9	
	ASESS	448.1	152.3	110.4	20.3			456.6	132.3	
	MP <sup>19</sup>	452	150	107	20			454	132	
MgF <sub>2</sub>	Exp. <sup>33</sup>	497.4	164.0	112.2	-23.6			499.1	147.4	
	OHESS	126.6	82.7	59.8				192.7	48.6	91.9
	ULICS	133.9	85.7	60.4				191.2	50.4	90.5
	ASESS	126.6	82.7	58.7				193.7	52.0	89.7
	MP <sup>19</sup>	190	60	60				134	51	89
	Exp. <sup>37</sup>	123.7	73.2	53.6				177.0	55.2	

TABLE VIII. The calculated elastic constants for the the orthorhombic TiSi<sub>2</sub> and monoclinic ZrO<sub>2</sub> using OHESS, ASESS, and ULICS, in comparison with MP data and with experiments

System	Method	$C_{11}$	$C_{12}$	$C_{13}$	$C_{15}$	$C_{22}$	$C_{23}$	$C_{25}$	$C_{33}$	$C_{35}$	$C_{44}$	$C_{46}$	$C_{55}$	$C_{66}$
ZrO <sub>2</sub>	OHESS	285.1	141.0	85.3	41.5	308.0	122.2	-0.8	225.6	2.9	65.2	-6.2	79.7	112.2
	ULICS	328.5	140.3	111.0	36.0	313.0	125.7	13.5	270.0	-5.1	55.0	0.43	72.1	104.1
	ASESS	285.1	141.0	86.3	42.1	307.6	123.5	-0.5	231.6	2.7	71.3	-7.4	82.4	115.2
	MP <sup>19</sup>	256	140	99	-1	357	152	3	301	-40	114	8	80	70
	Exp. <sup>38</sup>	361	142	55	-21	408	196	31	258	-18	100	-23	81	126
TiSi <sub>2</sub>	OHESS	321.5	33.1	90.3		322.5	37.8		401.2		71.6		101.4	112.9
	ULICS	319.1	34.2	89.4		313.9	36.6		402.5		73.1		104.3	113.5
	ASESS	321.5	33.1	90.2		322.5	32.9		413.4		73.5		104.8	114.4
	MP <sup>19</sup>	310	31	90		389	25		307		72		104	113
	Exp. <sup>39</sup>	320.4	29.3	86.0		317.5	38.4		413.2		75.8		112.5	117.5

TABLE IX. The calculated elastic constants for the the triclinic ReS<sub>2</sub> using OHESS, ASESS, and ULICS.

System	Method	$C_{11}$	$C_{12}$	$C_{13}$	$C_{14}$	$C_{15}$	$C_{16}$	$C_{22}$
ReS <sub>2</sub>	OHESS	215.5	43.2	2.7	-0.1	0.1	2.5	212.8
	ULICS	215.0	44.0	4.2	-0.5	-0.6	2.3	213.7
	ASESS	215.5	43.2	2.7	-0.1	0.1	2.5	212.8
		$C_{23}$	$C_{24}$	$C_{25}$	$C_{26}$	$C_{33}$	$C_{34}$	$C_{35}$
	OHESS	2.5	-0.1	0.0	2.3	6.9	-0.1	0.0
	ULICS	4.3	0.4	-0.3	1.9	8.0	0.2	-0.3
	ASESS	2.5	-0.1	0.0	2.3	6.9	-0.1	0.0
		$C_{36}$	$C_{44}$	$C_{45}$	$C_{46}$	$C_{55}$	$C_{56}$	$C_{66}$
	OHESS	0.0	1.0	-0.1	0.0	0.8	0.0	76.8
	ULICS	-0.4	1.1	-0.2	-0.1	0.6	0.2	77.0
	ASESS	0.0	1.0	-0.1	0.0	0.8	0.0	76.8

the elastic constants calculations were performed on the hardware platform with the two CPUs of Xeon E5-2683

(2.0 GHz and 28 cores in total). We gathered the time data used for all the calculations of the 3D and 2D elastic constants and listed them in Table XI. From Table XI we note that the time used by OHESS, ULICS and ASESS for calculating elastic constants varies significantly, although they have the same level of accuracy.

In order to clearly compare the computation efficiency of the three strain sets, we plotted the ratios of time used by ULICS and ASESS with respective to OHESS in Fig. 2. It is clearly shown that the OHESS have overall the highest computation efficiency among the three strain sets used. For most of the 3D crystal systems tested, the OHESS has more than twice the efficiency of the ULICS or ASESS. While, except for the graphene and 2D-MoS<sub>2</sub> the OHESS nearly has the same efficiency compared with ULICS and ASESS. The number of strain sets in ASESS is always 6 for 3D and 3 for 2D (see Table III), and naturally the ASESS has relatively lower efficiency. While

TABLE X. The 2D in-plane elastic constants (N/m) of various 2D materials in comparison with others' calculations. O, U, and A represent OHES, ULICS, and ASESS, respectively.

Systems	$C_{11}$		$C_{12}$		$C_{22}$		$C_{66}$	
	Our work	Ref.	Our work	Ref.	Our work	Ref.	Our work	Ref.
Phosphorene	103.4 <sup>[O]</sup>	105.2 <sup>40</sup>	18.0 <sup>[O]</sup>	18.4 <sup>40</sup>	24.6 <sup>[O]</sup>	26.2 <sup>40</sup>	21.8 <sup>[O]</sup>	22.4 <sup>40</sup>
	110.6 <sup>[U]</sup>	104.4 <sup>20</sup>	13.8 <sup>[U]</sup>	21.6 <sup>20</sup>	28.6 <sup>[U]</sup>	34.0 <sup>20</sup>	24.3 <sup>[U]</sup>	27.4 <sup>20</sup>
	104.1 <sup>[A]</sup>		17.4 <sup>[A]</sup>		24.6 <sup>[A]</sup>		22.8 <sup>[A]</sup>	
AuSe	34.1 <sup>[O]</sup>		2.7 <sup>[O]</sup>		9.3 <sup>[O]</sup>		3.3 <sup>[O]</sup>	
	34.9 <sup>[U]</sup>		2.5 <sup>[U]</sup>		9.4 <sup>[U]</sup>		3.3 <sup>[U]</sup>	
	34.2 <sup>[A]</sup>		2.7 <sup>[A]</sup>		9.3 <sup>[A]</sup>		3.3 <sup>[A]</sup>	
Graphene	353.2 <sup>[O]</sup>	358.1 <sup>40</sup>	63.7 <sup>[O]</sup>	60.4 <sup>40</sup>				
	353.2 <sup>[U]</sup>	349.1 <sup>20</sup>	64.2 <sup>[U]</sup>	60.3 <sup>20</sup>				
	353.2 <sup>[A]</sup>		63.9 <sup>[A]</sup>					
MoS <sub>2</sub>	136.9 <sup>[O]</sup>	131.4 <sup>40</sup>	33.1 <sup>[O]</sup>	32.6 <sup>40</sup>				
	137.1 <sup>[U]</sup>	128.9 <sup>20</sup>	33.3 <sup>[U]</sup>	32.6 <sup>20</sup>				
	136.9 <sup>[A]</sup>		33.7 <sup>[A]</sup>					
FeSe	58.2 <sup>[O]</sup>		22.7 <sup>[O]</sup>		38.1 <sup>[O]</sup>			
	57.6 <sup>[U]</sup>		22.5 <sup>[U]</sup>		38.3 <sup>[U]</sup>			
	58.4 <sup>[A]</sup>		22.3 <sup>[A]</sup>		38.2 <sup>[A]</sup>			

TABLE XI. The computation time used by the three kinds of strain sets, OHES, ULICS and ASESS. The time is in second.

Dimensional	Strain sets	Diamond	Al	CsCl	Os	Ti	TiSi <sub>2</sub>
3D	OHES	222	392	196	555	218	2317
	ULICS	452	1483	701	1225	773	4993
	ASESS	956	2556	946	1605	640	2811
		MgF <sub>2</sub>	Al <sub>2</sub> O <sub>3</sub>	CaMg(CO <sub>3</sub> ) <sub>2</sub>	ZrO <sub>2</sub>	TiB <sub>2</sub>	CaMoO <sub>4</sub>
	OHES	3580	7074	22200	27474	401	17207
	ULICS	6720	14958	32385	48593	1196	21955
2D	ASESS	4687	22260	67936	25703	1165	36681
		ReS <sub>2</sub>	2D-FeSe	Graphene	Phosphorene	2D-MoS <sub>2</sub>	2D-AuSe
	OHES	59701	3898	404	5396	2298	17860
	ULICS	80100	3662	749	7858	2278	21916
	ASESS	59701	4847	1580	6545	6311	18974

the OHES and ULICS have nearly the same number of strain sets except for the monoclinic crystal system and they have exactly the same number of strain sets except for the triclinic crystal system (see Table IV). The reason for the low efficiency of the ULICS is in that it lowers the symmetry of crystal by using the coupled strain sets and then lengthens the time for calculating the stresses by VASP.

### C. Discussions

We systematically tested and compared the accuracy and computation efficiency of elastic constants using the three kinds of strain matrix sets, the OHES, the ULICS, and the ASESS for both 3D and 2D systems. For the 3D systems, the test cases cover the seven crystal systems ranging from the cubic to the triclinic systems. The 2D tests include the square, hexagonal, and rectangular systems except the oblique system. Although the three kinds of strain sets have the same level of accuracy in

calculating elastic constants, the OHES has the highest computation efficiency. This is especially apparent for the crystal systems with higher symmetry, such as cubic and hexagonal (Diamond, Al, CsCl, Os, Ti, TiB<sub>2</sub> as shown in Fig.2). While, the advantage of OHES decreases relative to ULICS and ASESS with the decrease of the symmetry of crystal system. This can be attributed to two facts: the first is that the test cases have originally lower symmetries before applying the OHES or the ULICS strain sets, and then differ not so much as higher symmetry crystal systems after applying the two strain sets. The second one is that the number of strain sets used in the OHES approach to that of ASESS. Hence, the efficiency advantage of OHES have slightly decrease with respect to ULICS and ASESS.

As for the 2D case, the OHES has smaller advantages over the ULICS in computation efficiency. This is mainly because of the low symmetry of original 2D lattice. And the OHES keeps almost the same symmetry with the ULICS after applying strains to crystal lattice. But the OHES is much more efficient than ASESS in some cases,

for instance the the graphene and the 2D MoS<sub>2</sub>, resulted from the small number of strain sets in the OHES.

#### IV. CONCLUSIONS

In summary, we proposed the optimized high efficiency strain-matrix sets (OHES) to calculate the elastic constants according to the stress-strain relation originally defined in Hooke's law. After extensive test and comparison of the OHES with the ULICS and ASESS in the computation accuracy and efficiency, we conclude that the OHES is the most efficient one to calculate elastic in both the 3D and 2D cases at the same level of computational accuracy. Therefore, the OHES will greatly

improve the computational efficiency of elastic constants using the stress-strain in future. This is very helpful for the quick examination of the stability of new crystal structures in the new materials design, especially in constructing the elastic constant database like MP elastic database<sup>19</sup>.

#### V. ACKNOWLEDGMENTS

We acknowledge the supports from National Natural Science Foundation of China (41574076), the Key Research Scheme of Henan Universities (18A140024), and the Research Scheme of LYNU Innovative Team under Grant No. B20141679.

- 
- \* zliu@163.com
- <sup>1</sup> A. M. Tehrani and J. Brgoch, *J. Solid State Chem.* **271**, 47 (2019).
  - <sup>2</sup> T. Lay and T. C. Wallace, *Modern Global Seismology* (Elsevier Inc., Amsterdam, 1995).
  - <sup>3</sup> N. W. Ashcroft and N. D. Mermin, *Solid State Physics* (Harcourt College Publishers, New York, 1976).
  - <sup>4</sup> K. Tatsumi, I. Tanaka, K. Tanaka, H. Inui, M. Yamaguchi, H. Adachi, and M. Mizuno, *J. Phys.: Condens. Matter* **15**, 6549 (2003).
  - <sup>5</sup> P. Hohenberg and W. Kohn, *Phys. Rev.* **136**, B864 (1964).
  - <sup>6</sup> W. Kohn and L. J. Sham, *Phys. Rev.* **140**, A1133 (1965).
  - <sup>7</sup> Z. L. Liu, *Comput. Phys. Commun.* **185**, 1893 (2014).
  - <sup>8</sup> Y. Wang, J. Lv, L. Zhu, and Y. Ma, *Phys. Rev. B* **82**, 094116 (2010).
  - <sup>9</sup> Y. Wang, J. Lv, L. Zhu, and Y. Ma, *Comput. Phys. Commun.* **183**, 2063 (2012).
  - <sup>10</sup> C. W. Glass, A. R. Oganova, and N. Hansen, *Comput. Phys. Commun.* **175**, 713 (2006).
  - <sup>11</sup> C. J. Pickard and R. J. Needs, *J. Phys.: Condens. Matter* **23**, 053201 (2011).
  - <sup>12</sup> D. C. Lonie and E. Zurek, *Comput. Phys. Commun.* **182**, 372 (2011).
  - <sup>13</sup> Z. J. Wu, E. J. Zhao, H. P. Xiang, X. F. Hao, X. J. Liu, and J. Meng, *Phys. Rev. B* **76**, 054115 (2007).
  - <sup>14</sup> F. Mouhat and F. X. Coudert, *Phys. Rev. B* **90**, 224104 (2014).
  - <sup>15</sup> J. F. Nye, *Physical Properties of Crystals* (Oxford University Press, Oxford, 1985).
  - <sup>16</sup> M. Born and K. Huang, *Dynamical Theory of Crystal Lattices* (Oxford University Press, Oxford, 1954).
  - <sup>17</sup> Z. L. Liu, H. Jia, R. Li, X. L. Zhang, and L. C. Cai, *Phys. Chem. Chem. Phys.* **19**, 13219 (2017).
  - <sup>18</sup> R. Yu, J. Zhu, and H. Q. Ye, *Comput. Phys. Commun.* **181**, 671 (2010).
  - <sup>19</sup> M. D. Jong, W. Chen, T. Angsten, A. Jain, R. Notestine, A. Gamst, M. Sluiter, C. K. Ande, S. van der Zwaag, J. J. Plata, C. Toher, S. Curtarolo, G. Ceder, K. A. Persson, and M. Asta, *Scientific Data* **2**, 150009 (2015).
  - <sup>20</sup> V. Wang, N. Xu, J. C. Liu, G. Tang, and W. T. Geng, "Vaspkit: A pre- and post-processing program for vasp code (arXiv:1908.08269v2)," (2019).
  - <sup>21</sup> R. Golezorkhtabar, P. Pavone, J. Spitaler, P. Puschnig, and C. Draxl, *Comput. Phys. Commun.* **184**, 1861 (2013).
  - <sup>22</sup> W. F. Perger, J. Criswell, B. Civalleri, and R. Dovesi, *Comput. Phys. Commun.* **180**, 1753 (2009).
  - <sup>23</sup> G. V. Sinko and N. A. Smirnov, *J. Phys.: Condens. Matter* **14**, 6989 (2002).
  - <sup>24</sup> W. Voigt, *Lehrbuch Der Kristallphysik, Mit Ausschluss Der Kristalloptik* (Leipzig, Berlin, 1928).
  - <sup>25</sup> P. E. Blöchl, *Phys. Rev. B* **50**, 17953 (1994).
  - <sup>26</sup> G. Kresse and D. Joubert, *Phys. Rev. B* **59**, 1758 (1999).
  - <sup>27</sup> G. Kresse and J. Furthmüller, *Phys. Rev. B* **54**, 11169 (1996).
  - <sup>28</sup> J. P. Perdew, K. Burke, and M. Ernzerhof, *Phys. Rev. Lett.* **78**, 1396 (1997).
  - <sup>29</sup> H. J. McSkimin and J. Andreatch, *J. Appl. Phys.* **43**, 2944 (1972).
  - <sup>30</sup> D. D. Slagle and H. A. McKinstry, *J. Appl. Phys.* **38**, 446 (1967).
  - <sup>31</sup> R. M. Hazen, L. W. Finger, and J. W. E. Mariathasan, *J. Phys. Chem. Solids* **46**, 253 (1985).
  - <sup>32</sup> C. Pantea, I. Stroe, H. Ledbetter, J. B. Betts, Y. Zhao, L. L. Daemen, H. Cynn, and A. Migliori, *Phys. Rev. B* **80**, 024112 (2009).
  - <sup>33</sup> C. Smithells, E. Brandes, and F. Institute, *Smithells Metals Reference Book*, Vol. 8 (Butterworth-Heinemann, 1983).
  - <sup>34</sup> P. S. Spoor, J. D. Maynard, M. J. Pan, D. J. Green, J. R. Hellman, and T. Tanaka, *Appl. Phys. Lett.* **70**, 1959 (1997).
  - <sup>35</sup> P. Humbert and F. Plique, *C. R. Acad. Sci. Paris* **275**, 391 (1972).
  - <sup>36</sup> W. J. Alton and A. J. Barlow, *J. Appl. Phys.* **38**, 3817 (1967).
  - <sup>37</sup> H. R. Cutler, J. J. Gibson, and K. A. McCarthy, *Solid State Commun.* **6**, 431 (1968).
  - <sup>38</sup> S. C. Chan, Y. Fang, M. Grimsditch, Z. Li, M. Nevitt, W. Robertson, and E. S. Zoubolis, *J. Am. Ceram. Soc.* **74**, 1742 (1991).
  - <sup>39</sup> M. Nakamura, *Metall. Trans. A* **25A**, 331 (1993).
  - <sup>40</sup> L. Wang, A. Kutana, X. Zou, and B. I. Yakobson, *Nanoscale* **7**, 9746 (2015).